Histological tumor necrosis in pancreatic cancer after neoadjuvant therapy

MASASHI KUDO[1,2], GENICHIRO ISHII[1], NAOTO GOTOHDA[2], MASARU KONISHI[2], SHINICHIRO TAKAHASHI[2,3], SHIN KOBAYASHI[2], MOTOKAZU SUGIMOTO[2], JOHN D. MARTIN[4], HORACIO CABRAL[5] and MOTOHIRO KOJIMA[1]

[1]Division of Pathology, Exploratory Oncology Research and Clinical Trial Center, National Cancer Center; [2]Department of Hepatobiliary and Pancreatic Surgery, and [3]Clinical Research Support Office, National Cancer Center Hospital East, Kashiwa, Chiba 277-8577; [4]NanoCarrier Co., Ltd. Kashiwa, Chiba 277-0882; [5]Department of Bioengineering, Graduate School of Engineering, The University of Tokyo, Tokyo 113-8656, Japan

Received January 7, 2022; Accepted April 6, 2022

DOI: 10.3892/or.2022.8332

Abstract. The pathological prognostic factors in pancreatic cancer patients who have received neoadjuvant therapy (NAT) are still elusive. The aim of the present study was to investigate the prognostic potential of histological tumor necrosis (HTN) in patients who received NAT and to evaluate tumor changes after NAT. HTN was studied in 44 pancreatic cancer patients who received NAT followed by surgery (NAT group) compared with 263 patients who received upfront surgery (UFS group). The prognostic factors in the NAT group were analyzed, and carbonic anhydrase 9 (CA-9) expression was compared between the NAT and USF group to evaluate the hypoxic microenvironment changes during NAT. HTN was found in 15 of 44 patients in the NAT group, and its frequency was lower than that in the UFS group (34 vs. 51%, P=0.04). Cox proportional hazards models identified HTN as an independent risk factor for relapse-free survival in the NAT group [risk ratio (RR), 5.60; 95% confidence interval (CI): 2.27-14.26, P<0.01]. Significant correlations were found between HTN and CA-9 expression both in the NAT and UFS groups (P<0.01 for both). CA-9 expression was significantly upregulated in the NAT group overall, although this upregulation was specifically induced in patients without HTN. In conclusion, HTN was a poor prognostic factor in pancreatic cancer patients receiving NAT followed by surgery, and the present study suggests a close association between HTN and tumor hypoxia. Increased hypoxia after NAT may support the thesis for re-engineering the hypoxia-alleviating tumor microenvironment in NAT regimens for pancreatic cancer.

Correspondence to: Dr Motohiro Kojima, Division of Pathology, Exploratory Oncology Research and Clinical Trial Center, National Cancer Center, 6-5-1, Kashiwa-no-ha, Kashiwa, Chiba 277-8577, Japan
E-mail: mokojima@east.ncc.go.jp

Abbreviations: CA-9, carbonic anhydrase 9; CI, confidence interval; DSS, disease-specific survival; HTN, histological tumor necrosis; NAT, neoadjuvant therapy; PEAs, poorly enhanced areas; RFS, relapse-free survival; RR, risk ratio; UFS, upfront surgery

Key words: biomarker, necrosis, pancreatic carcinoma, prognosis, hypoxia

Introduction

Pancreatic cancer is one of the most aggressive malignancies with a dismal prognosis, and the 5-year overall survival rate is 8% (1). Even after radical surgery, the prognosis of pancreatic cancer remains poor owing to the high rate of local recurrence and/or distant metastasis, with an estimated median survival after surgery of only 16.8 months (2). Recently, survival benefit from neoadjuvant therapy (NAT) in patients with pancreatic cancer has been reported, and surgical resection after NAT is the current standard treatment for patients with resectable or borderline resectable pancreatic cancer (2-4). Therefore, histological biomarker research in pancreatic cancer after NAT is important for understanding treatment resistance and for predicting prognosis.

Histological tumor necrosis (HTN) is a potential predictor of a poor prognosis. In particular, we previously reported that the size of HTN is strongly correlated with postoperative prognosis in resectable pancreatic cancer without NAT (5-7). Moreover, the hypoxic microenvironment of the tumor, represented by overexpression of carbonic anhydrase 9 (CA-9), was found to be closely linked with the formation of HTN in pancreatic cancer patients without NAT (7). On the other hand, the utility of these physiological tumor conditions as prognostic factors and their alteration during NAT have not been investigated in human pancreatic cancer tissue. Comparison of physiological tumor conditions in pancreatic cancer with or without NAT may allow us to determine physiological alterations during NAT and may provide basic information to establish new treatment strategies targeting them. Thus, the aim of this study was to investigate the prognostic potential of HTN after NAT, and

to measure the alterations in tumor hypoxia after NAT in pancreatic cancer.

Patients and methods

Patients. From January 2011 to December 2018, 339 patients underwent pancreatectomy for pancreatic cancer at the National Cancer Hospital East, Kishiwa, Japan. Of the 339 patients, 32 were excluded for recurrent pancreatic cancer in the remnant pancreas (n=18) or inconsistent patient information (n=14). The remaining 307 patients were investigated in this study. According to the clinical practice guidelines for pancreatic cancer from the Japan Pancreas Society (8), single-agent S-1 was given as standard adjuvant chemotherapy except for patients who received systemic chemotherapy due to early recurrence or who refused standard adjuvant chemotherapy. This retrospective study was approved by the National Cancer Ethics Review Board (reference 2017-328).

Radiologic criteria for resectability. The staging and resectability of the pancreatic cancer cases were assessed with contrast-enhanced computed tomography imaging, magnetic resonance imaging, and ultrasound. The patient data were reviewed by hepato-biliary-pancreatic surgeons, medical oncologists, and radiologists during a conference to determine tumor staging and resectability. Local tumor extent was categorized as potentially resectable, borderline resectable, or locally advanced. The criteria for borderline resectable disease were defined based on the General Rules for the Study of Pancreatic Cancer edited by the Japan Pancreatic Society (9) as follows: a) contact with the celiac artery <180˚ without deformity or narrowing; b) any contact with the common hepatic artery without contact with the celiac artery or proper hepatic artery; c) contact with the superior mesenteric artery <180˚ without deformity or narrowing; and/or d) contact with the portal-superior mesenteric vein ≥180˚ without caudal extensions over the level of the inferior end of the duodenum. Any tumors with vascular contact exceeding any of the above borderline resectable criteria were determined to be locally advanced disease.

In accordance with the treatment algorithm based on the General Rules of Pancreatic Cancer edited by the Japan Pancreatic Society (9), patients with diagnosed resectable disease underwent upfront surgery (UFS), whereas patients who had diagnosed borderline resectable disease received NAT followed by radical surgery. If patients satisfied the eligibility criteria of clinical trials (10-12), they participated in these clinical trials of NAT for resectable and borderline resectable pancreatic cancer.

NAT. During the study period, neoadjuvant strategies included systemic induction chemotherapy or locoregional chemoradiation. Neoadjuvant systemic chemotherapy regimens included gemcitabine/nab-paclitaxel, gemcitabine/S-1, and single-agent S-1. Chemoradiation used S-1 with concurrent radiation therapy (RT) with a total dosage of 50.4 Gy in 28 fractions. If upon restaging after completion of NAT, the patient was surgically fit and the extent of the disease remained potentially resectable or borderline resectable without distant metastasis, operative exploration was indicated.

Histological analysis of surgical specimens. Histological characteristics, such as tumor area, tumor grade, tumor size, lymph node metastasis, microvascular invasion, neural invasion, and HTN, were compared between the UFS and NAT groups. Moreover, morphological features of HTN, such as necrotic area, necrotic area/tumor area, perimeter, circularity, number of necroses, number of ruptured cancer glands, neutrophil infiltration, and collagen bundles, were compared between the two groups to evaluate the alterations after NAT in pancreatic cancer.

All tumor tissues were fixed in 10% formalin neutral buffer solution for two days at 20˚C, sliced at 4- to 7-mm intervals, and all slices with tumor were submitted for microscopic examination. Then, 4-μm-thick sections were stained with hematoxylin (30011; FUJIFILM Wako Pure Chemical Corp.) for 3 min and eosin (0.5%, 32012; FUJIFILM Wako Pure Chemical Corp.) for 5 min at room temperature, and all hematoxylin and eosin (H&E)-stained slides from the largest slice with tumor that was determined during the histologic assessment were digitally scanned in each case. The H&E sections were scanned using the NanoZoomer 2.0 system (Hamamatsu Photonics), and morphological and histological analysis was performed by a single investigator (MJ, with more than 23 years of experience examining pancreatic histology) without any radiological or clinical information.

The definition of HTN was based on previous reports (5-7). HTN was assessed only as lesions including preserved cell outlines without nuclei. Both confluent cell death in an invasive area (visible at an objective lens magnification of x4) and smaller areas of necrosis were regarded as necrotic. Death of many confluent cells in an invasive area included ruptured cancer glands (Fig. 1A) and collagen bundles (Fig. 1B). Intraluminal necrosis that did not extend to the stroma was not regarded as necrosis (Fig. 1C). The investigator could determine the borderline between HTN and other tissues for assessing the size of HTN, referencing confluent cell death, ruptured cancer glands, and collagen bundles, while blind to clinical information. After determination of the HTN regions, the ruler function in NanoZoomer 2.0 was used to evaluate the size of HTN (Fig. S1, red line). When multiple regions of HTN were present, the largest area of HTN was selected as representative of that case. However, tumor necrosis after neoadjuvant therapy was more confusing, because the area of tumor cells may vanish completely after therapy. Therefore, lesions including preserved cell outlines without nuclei were considered to be indicative of tumor necrosis. The size of HTN was measured and classified into small (maximum diameter <5 mm, Fig. 1D) and large necrosis (maximum diameter >5 mm, Fig. 1E) to investigate the size-dependent features of HTN. The cut-off value (5 mm) of this size classification was calculated in our previous report (5). The circularity of HTN was calculated as follows: $4 \pi \times (\text{area of necrosis})/(\text{perimeter of necrosis})^2$. Measurement of the tumor area was based on our previous reports (5,13). The pathological stage of patients was defined according to the TNM stage in the 8th Union for International Cancer Control staging system (14).

Histological features associated with neoadjuvant therapeutic effects were assessed using the College of American Pathologists (CAP) regression grading system and Evans grading system (15,16). The CAP grading system was assessed

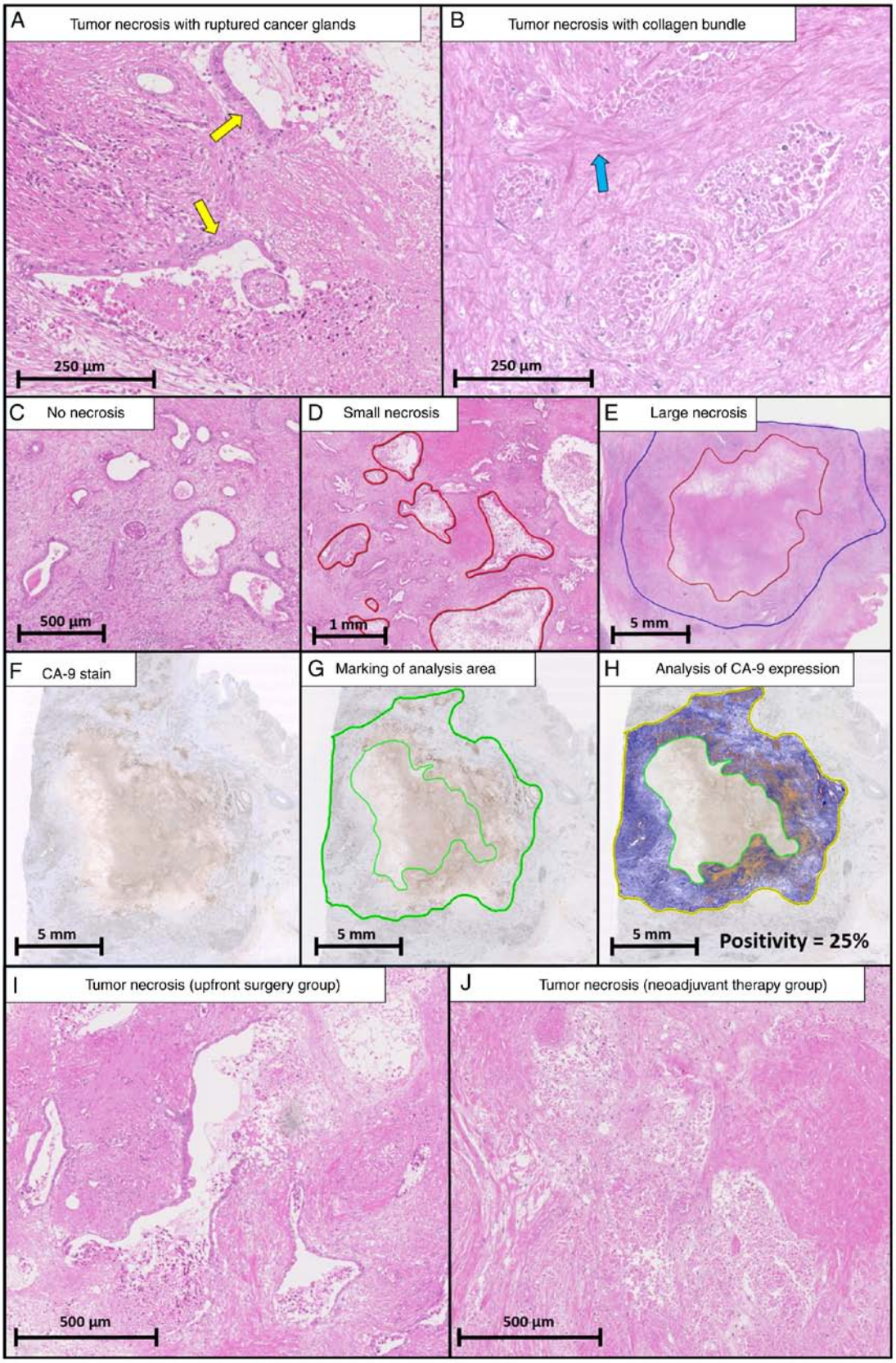

Figure 1. Histological tumor necrosis is often accompanied by ruptured cancer glands (A, yellow arrows) and collagen bundles (B, blue arrow). The regions of the tumor and of tumor necrosis are encircled by blue and red lines, respectively (C-E). The definition of the size of necrosis in pancreatic ductal adenocarcinoma according to maximum diameter. Histological tumor necrosis is absent or limited in a cancer gland (C). Necrosis with a maximum diameter less than 5 mm is defined as small necrosis, as indicated by red lines (D). Necrosis with a maximum diameter greater than 5 mm is defined as large necrosis, as indicated by a red line. The tumor area is marked by a blue line (E). Immunohistochemical detection of expression of CA-9 (F). The regions of the tumor area without necrosis are encircled within the two areas denoted by green lines (G). CA-9 positivity was calculated as the percentage of CA-9-positive pixels of the entire pixel count using morphometric analysis with a positive pixel count algorithm (Aperio ImageScope, version 12.4; Leica Biosystems) (H). The representative tumor necrosis of the upfront surgery group includes many ruptured cancer glands (I). On the other hand, the tumor necrosis of the neoadjuvant therapy group includes many collagen bundles, but no ruptured cancer glands (J). CA-9, carbonic anhydrase 9.

as follows: Grade 0, no viable cancer cells; grade 1, single cells or rare small groups of cancer cells; grade 2, residual tumor with evident tumor regression; and grade 3, extensive residual tumor with no evident tumor regression (15). The Evans grading system was assessed as follows: grade 1, <10% to no tumor cells destroyed; grade 2a, 10 to 50% of tumor cells destroyed; grade 2b, 51 to 90% of tumor cells destroyed; grade 3, few (<10%) tumor cells present; and grade 4, no viable tumor cells (16).

Immunohistochemical analysis of surgical specimens. Hypoxic microenvironment status, represented by CA-9, was compared between UFS and NAT groups to evaluate the alterations in physiological tumor conditions after NAT in pancreatic cancer.

Immunohistochemistry was performed on 10% formalin neutral buffer solution-fixed, paraffin-embedded tissue sections by Ventana autostainer model Discover XT (Ventana Medical System. A polyclonal goat antibody against human CA-9 antibody (1:300, sc-365900; Santa Cruz Biotechnology, Inc.) was used. In brief, tissue sections were incubated in citrate buffer for 4 min at 72˚C to retrieve antigenicity, followed by incubation with the primary antibody. The bound primary antibody was incubated with the anti-goat secondary antibody at 37˚C for 8 min and visualized using ultraView Universal DAB Detection Kit (760-500; Roche Diagnostics). The CA-9 sections were scanned using the NanoZoomer 2.0 system (Fig. 1F). The tumor regions without necrosis were encircled to evaluate the hypoxic tumor microenvironment status (Fig. 1G) and quantified using morphometric analysis from a color-detecting algorithm. CA-9 positivity was calculated as the percentage of CA-9-positive pixels out of the entire pixel count using morphometric analysis with the positive pixel count algorithm (Aperio ImageScope, version 12.4; Leica Biosystems) (Fig. 1H) (17).

Statistical analysis. Categorical variables were evaluated using the Chi-squared test and are presented as numbers and percentages, whereas continuous variables were evaluated using the Mann-Whitney U test and are presented as medians and ranges. Relapse-free survival (RFS) and disease-specific survival (DSS) rates were calculated with the Kaplan-Meier method, and differences were compared with the log-rank test. RFS and DSS were defined as the interval from the date of starting first treatment (UFS or NAT) to the date of recurrence or disease-specific death due to pancreatic cancer, respectively, or the date censored at the last follow-up. The observation period was until the end of September 2019, and the median duration was 24.5 months [95% confidence interval (CI), 20.3-31.1]. Univariate and multivariate analyses of prognostic factors were performed using a Cox proportional hazards model. The factors that were found to be significant on univariate analyses in the UFS group were included in the multivariate analysis, the results of which are presented as risk ratios (RRs) and 95% CIs. However, multivariate analyses of prognostic factors in the NAT group were not performed due to the small sample size. All P-values were based on two-sided statistical tests, and the significance level was set at 0.05. Statistical analyses were performed using JMP (version 12.0.10; SAS Institute).

Results

Clinical and histological characteristics of the patients. Of the 307 patients who were reviewed, 44 (14%) received NAT followed by radical surgery (NAT group), and 263 (86%) underwent UFS (UFS group). Table I shows a comparison of the clinical and histological variables between the NAT group and UFS group at baseline. Of the clinical characteristics, patient mean age was significantly higher in the UFS group than that in the NAT group (70 vs. 67 years, P=0.009), and the frequency of borderline resectable pancreatic cancer was significantly lower in the UFS group than in the NAT group (1 vs. 66%, P<0.001). As for the histological characteristics, the frequencies of lymph node metastasis (65 vs. 34%, P<0.001), lymphatic invasion (74 vs. 52%, P<0.001), venous invasion (92 vs. 80%, P=0.014), and neural invasion (95 vs. 86%, P=0.039) were significantly lower in the NAT group than in the UFS group. Of note, in comparison with the UFS group, the frequency of HTN (51 vs. 34%, P=0.043) was significantly lower in the NAT group. On the other hand, the frequency of large histological necrosis was comparable in the UFS and NAT groups.

Histological findings of necrosis. Comparison of HTN between the NAT and UFS groups is shown in Table II. In the NAT group, the number of ruptured cancer glands was significantly lower (P=0.017), and the rate of collagen bundles was significantly higher (P=0.030) than in the UFS group. No differences in morphological variables, such as necrotic area, necrotic area/tumor area, perimeter, or circularity, were seen between the two groups. Representative areas of HTN in the NAT and UFS groups are shown in Fig. 1I and J.

Prognostic significance according to the size of necrosis. The prognostic significance of the size of necrosis is shown in Fig. 2. The median relapse-free survival (RFS) and disease-specific survival (DSS) in the UFS group of 263 patients were 17.2 and 56.4 months, respectively. For both RFS and DSS, significant size-dependent deterioration of the clinical prognosis was seen in the UFS group (Fig. 2A and B). The median RFS and DSS in the NAT group of 44 patients were 18.5 and 66.1 months, respectively. Kaplan-Meier curves of RFS and DSS were significantly different between no necrosis and large necrosis in the NAT group (P<0.01, Fig. 2C and D).

Risk analysis of prognostic factors in the NAT group. Univariate risk analyses of prognostic factors associated with DSS in the NAT group are shown in Table III. On univariate analyses, HTN was the only significant risk factor for DSS (RR, 11.94; 95% CI, 4.13-37.57; P<0.001), and large histological necrosis was a robust factor related to a poor prognosis (RR, 39.25; 95% CI, 9.54-267.97; P<0.001). Univariate risk analyses of prognostic factors associated with RFS in the NAT group are shown in Table IV. HTN was the only significant risk factor for RFS (RR, 6.40; 95% CI, 2.68-15.62; P<0.001), and large histological necrosis was a robust factor related to a poor prognosis (RR, 17.35; 95% CI, 5.71-58.92; P<0.001).

Correlation between CA-9 positivity and HTN. Of the 307 patients who were reviewed, paraffin-embedded tissue sections of two patients in the NAT group were not

Table I. Comparison of the clinicopathological characteristics between the UFS group and the NAT group.

Clinical characteristic	UFS group (n=263)	NAT group (n=44)	P-value
Age (years)	70 (43-87)	67 (38-78)	**0.009**
Sex, n (%)			
Male	159 (61)	28 (64)	0.689
Body mass index (kg/m^2)	21.4 (15.6-38.8)	22.3 (16.6-28.3)	0.183
Tumor location, n (%)			
Head	171 (65)	28 (64)	0.679
Body and tail	88 (33)	16 (36)	
Whole pancreas	4 (2)	0 (0)	
Clinical tumor size (before NAT), n (%)			
<20 mm	127 (48)	18 (41)	0.571
≥20, <40 mm	129 (49)	24 (55)	
≥40 mm	7 (3)	2 (5)	
Local tumor extent, n (%)			
Potentially resectable	260 (99)	15 (34)	**<0.001**
Borderline resectable	3 (1)	29 (66)	
NAT, n (%)			
S-1 + radiation	-	23 (52)	-
GEM + nabPTX	-	10 (23)	
GEM + S-1	-	10 (23)	
S-1 monotherapy	-	1 (2)	
Histological characteristics			
Tumor area (mm^2)	105 [10-513]	117 [4-309]	0.501
Tumor grade, n (%)			
Grade 1	44 (17)	13 (30)	0.120
Grade 2	196 (75)	27 (61)	
Grade 3	23 (9)	4 (9)	
Pathological tumor size, n (%)			
<20 mm	75 (29)	12 (27)	0.226
≥20, <40 mm	162 (62)	31 (71)	
≥40 mm	26 (10)	1 (2)	
Lymph node metastasis, n (%)			
Absence	91 (35)	29 (66)	**<0.001**
Presence	172 (65)	15 (34)	
Lymphatic invasion, n (%)			
Absence	68 (26)	21 (48)	**<0.001**
Presence	195 (74)	23 (52)	
Venous invasion, n (%)			
Absence	22 (8)	9 (20)	**0.014**
Presence	241 (92)	35 (80)	
Neural invasion, n (%)			
Absence	14 (5)	6 (14)	**0.039**
Presence	249 (95)	38 (86)	
Histological necrosis, n (%)			
Absence	130 (49)	29 (66)	**0.043**
Presence	133 (51)	15 (34)	
Histological large necrosis, n (%)			
Absence	210 (80)	33 (75)	0.464
Presence	53 (20)	11 (25)	

Categorical variables are presented as numbers and percentages, whereas continuous variables are presented as medians and range. Categorical variables were analyzed using the Chi-squared test, whereas continuous variables were analyzed using the Mann-Whitney test. Significant differences were found in age, clinical diagnosis, lymph node metastasis, lymphatic invasion, venous invasion, neural invasion, and necrosis between the upfront surgery group and the neoadjuvant therapy group. P-values representing significant differences are indicated in bold print. UFS, upfront surgery; NAT, neoadjuvant therapy; GEM, gemcitabine; nabPTX, nab-paclitaxel.

Table II. Comparison of histological tumor necrosis in patients with or without neoadjuvant therapy.

	Histological necrosis			Histological large necrosis		
	UFS group (n=133)	NAT group (n=5)	P-value	UFS group (n=53)	NAT group (n=11)	P-value
Necrotic area (mm^2)	10.3 [0.5-182.7]	46.4 (1.3-105)	0.139	68.6 [12.4-182.7]	54.4 (16.8-105.0)	0.428
Necrotic area/tumor area (%)	9 (1-82)	25 (1-56)	0.167	38 (4-82)	28 (16-56)	0.359
Perimeter (mm)	11.8 [2.8-65.4]	33.6 (3.5-46.9)	0.107	32.5 (16.6-65.4)	37.3 (17.7-46.9)	0.972
Circularity	0.66 [0.24-0.95]	0.58 (0.35-0.79)	0.117	0.62 (0.30-0.87)	0.51 (0.35-0.79)	0.251
Number of necroses	2 (1-22)	3 (1-8)	0.481	3 (1-9)	2 (1-5)	0.416
Number of ruptured cancer glands	5 (0-36)	2 (0-11)	**0.017**	15 (0-36)	2 (0-11)	**<0.001**
Neutrophil infiltration, n (%)						
Presence	37 (28)	3 (20)	0.518	16 (30)	2 (18)	0.420
Absence	96 (72)	12 (80)		37 (70)	9 (82)	
Collagen bundles, n (%)						
Presence	50 (38)	10 (67)	**0.030**	41 (77)	10 (91)	0.309
Absence	83 (62)	5 (33)		12 (23)	1 (9)	

Categorical variables are presented as numbers and percentages, whereas continuous variables are presented as medians and range. Categorical variables were analyzed using the Chi-squared test, whereas continuous variables were analyzed using the Mann-Whitney test. Significant differences were found in terms of the number of ruptured cancer glands and the presence of collagen bundles. P-values representing significant differences are indicated in bold print. UFS, upfront surgery; NAT, neoadjuvant therapy.

available. Thus, immunohistochemical analyses of CA-9 were performed in 305 patients. Histograms of CA-9 positivity for each patient in the UFS and NAT groups are shown in Fig. 3A and B, and the correlation between CA-9 positivity and HTN is able to be visualized in both the UFS and NAT groups. The median CA-9 positivity was higher in cases with than without HTN in the UFS group (23 vs. 10%, P<0.01), and a similar result was obtained in the NAT group (34 vs. 17%, P<0.01, Table SI). Moreover, predominant distribution of CA-9-positive tumor cells was frequently observed around HTN (Fig. 1G and H).

Comparisons of distributions with box plots of CA-9 positivity between the UFS and NAT groups are shown in Fig. 3C-E. Overall, the NAT group showed more prominent CA-9 positivity than the UFS group (22 vs. 14%, P=0.02, Fig. 3C). In patients without HTN, median CA-9 positivity was very low in the UFS group, whereas it was upregulated in the NAT Group (17% vs. 10%, P<0.01, Fig. 3D). On the other hand, in patients with HTN, median CA-9 positivity was high even in the UFS Group (23%) and was not upregulated in the NAT group (34%) (P=0.18, Fig. 3E). We hypothesized that CA-9 positivity is increased after NAT in all patients. However, baseline CA-9 expression in the UFS group was already correlated with HTN, and it was not significantly upregulated by NAT in patients with HTN.

Discussion

In the present study, first, the histological features of pancreatic cancer were compared between the upfront surgery (UFS) and neoadjuvant therapy (NAT) groups to estimate the morphological alteration of histological tumor necrosis (HTN) after NAT. The factors associated with a poor prognosis, such as lymph node metastasis, lymphatic invasion, venous invasion, neural invasion, and HTN, were significantly less frequent in the NAT group. Next, the risk factors for relapse-free survival (RFS) and disease-specific survival (DSS) were investigated, and it was found that HTN was a prognostic factor in the NAT group. Finally, the correlation between HTN and the hypoxic tumor microenvironment represented by CA-9 expression was investigated, and higher CA-9 positivity was found in cases with HTN in both the UFS and NAT groups.

The present study demonstrated drastic histological alterations after NAT. The frequency of HTN, lymph node metastasis, lymphatic invasion, venous invasion, and neural invasion in the NAT group was lower than that in the UFS group. Some reasons are as follows. First, NAT may reduce lymph node metastasis, vascular invasion, and HTN. A previous study reported that lymph node metastasis was significantly decreased after NAT, and some of these histological responses contribute to survival benefit in patients with

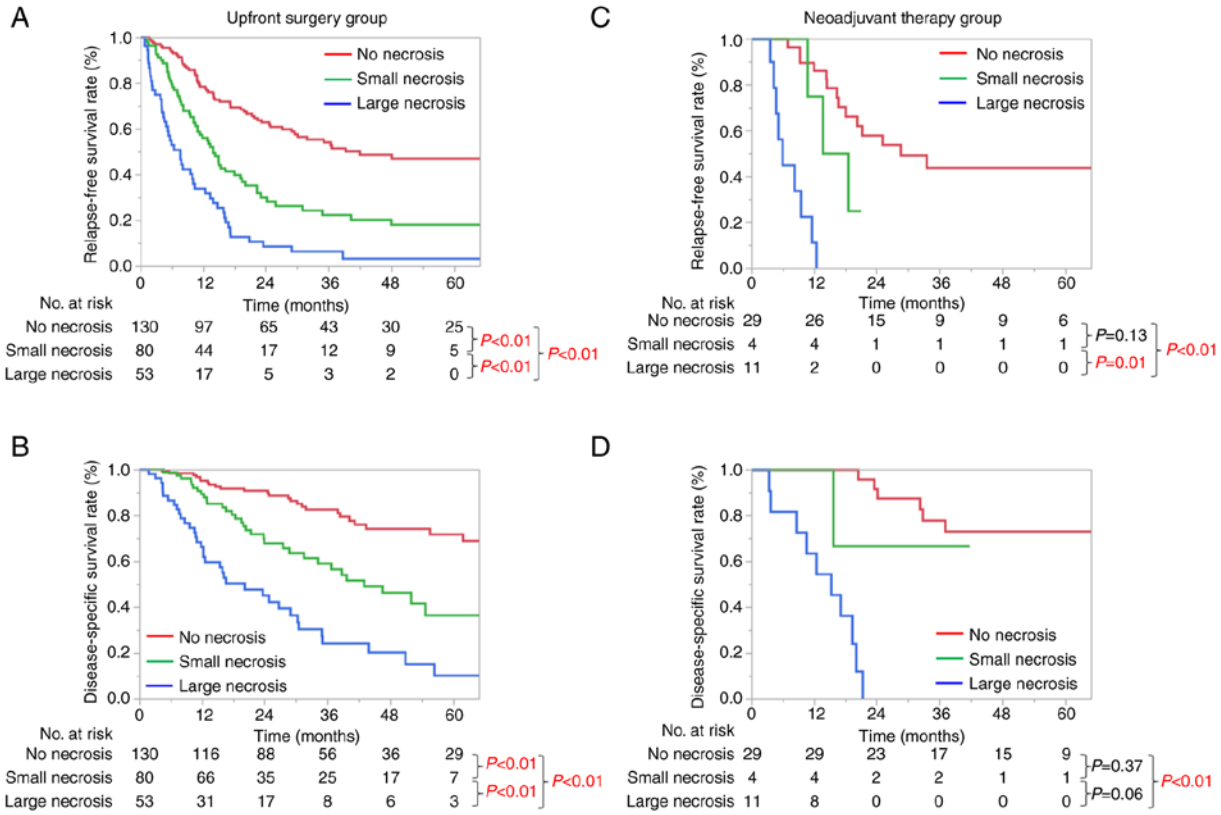

Figure 2. Kaplan-Meier estimates of relapse-free survival (A) and disease-specific survival (B) of the 263 patients in the upfront surgery group according to the size of necrosis. Kaplan-Meier estimates of relapse-free survival (C) and disease-specific survival (D) of the 44 patients in the neoadjuvant therapy group according to the size of necrosis. All Kaplan-Meier curves are significantly different among the three groups according to size of necrosis in the upfront surgery group. Kaplan-Meier curves are significantly different between no necrosis and large necrosis in the neoadjuvant therapy group.

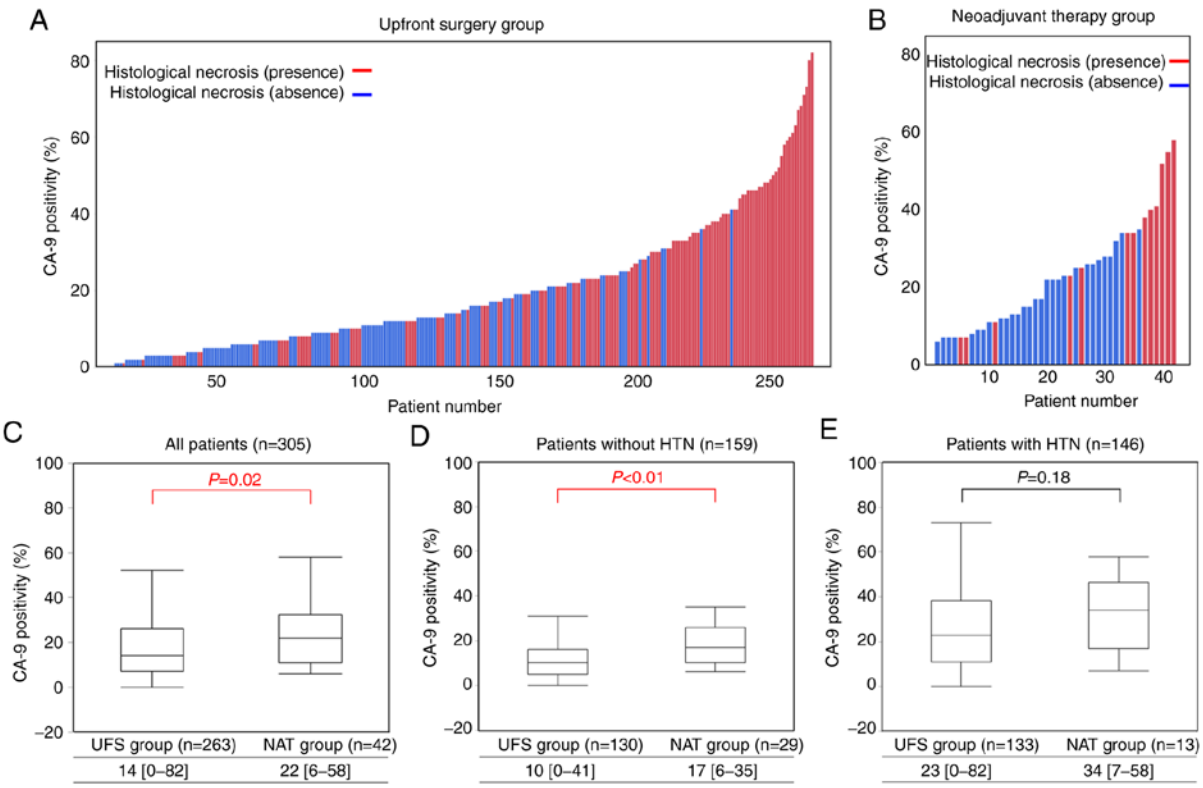

Figure 3. Histograms of CA-9 positivity in each patient in the upfront surgery group (A) and in the neoadjuvant therapy group (B). The correlation between CA-9 positivity and histological tumor necrosis is visualized in both groups. Comparisons of distributions of CA-9 positivity with box plots (%) between the UFS and NAT groups in all patients (C), patients without HTN (D), and patients with HTN (E). The difference between the UFS group and the NAT group was evaluated using pairwise comparison with the Mann-Whitney test. CA-9, carbonic anhydrase 9; NAT, neoadjuvant therapy; UFS, upfront surgery.

Table III. Univariate risk analyses of prognostic factors associated with DSS in the NAT group (n=44).

			Univariate analysis[a]	
Variable	n	Median DSS (months)	RR (95% CI)	P-value
Age (years)				
≥75	6	NR	0.41 (0.02-1.98)	0.316
<75	38	66.1		
Sex				
Male	28	66.1	1.10 (0.43-3.18)	0.841
Female	16	NR		
Body mass index (kg/m^2)				
≥25	8	NR	0.95 (0.34-3.37)	0.924
<25	36	66.1		
Local tumor extent				
Potentially resectable	15	37.0	1.25 (0.48-3.18)	0.639
Borderline resectable	29	66.1		
Tumor location				
Head	28	66.1	0.63 (0.24-1.61)	0.324
Body and tail	16	34.6		
Clinical tumor size (mm)				
≥20	24	32.2	2.66 (0.99-8.34)	0.053
<20	20	NR		
CA-9 before NAT (IU/ml)				
≥37	28	66.1	1.05 (0.39-2.68)	0.916
<37	16	NR		
Neoadjuvant therapy				
NAC+RT	23	66.1	0.77 (0.30-1.98)	0.578
NAC	21	32.7		
Pathological tumor size (mm)				
≥20	32	66.1	1.55 (0.55-5.49)	0.425
<20	12	NR		
Lymph node metastasis				
Positive	15	32.7	2.06 (0.78-5.24)	0.139
Negative	29	NR		
Lymphatic invasion				
Positive	23	32.2	1.38 (0.54-3.62)	0.496
Negative	21	66.1		
Vascular invasion				
Positive	35	32.1	1.86 (0.61-8.08)	0.299
Negative	9	66.1		
Perineural invasion				
Positive	38	66.1	1.98 (0.56-12.61)	0.324
Negative	6	NR		
CAP criteria				
Grade 1, 2	20	NR	0.40 (0.15-1.05)	0.063
Grade 3	24	32.2		
Evans criteria				
Grade 1	15	NR	0.80 (0.25-2.12)	0.659
Grade 2, 3	29	66.1		
Histological necrosis				
Positive	15	17.0	11.94 (4.13-37.57)	**<0.001**
Negative	29	NR		
Histological large necrosis				
Positive	11	15.2	39.25 (9.54-267.97)	**<0.001**
Negative	33	NR		

[a]Cox proportional hazards regression model. Upon univariate analysis, necrosis was considered a prognostic factor. P-values representing significant differences are indicated in bold print. DSS, disease-specific survival; CI, confidence interval; RR, risk ratio; CA-9, carbonic anhydrase 9; NAT, neoadjuvant therapy; RT, radiotherapy; CAP, College of American Pathologists.

Table IV. Univariate risk analyses of prognostic factors associated with RFS in the NAT group (n=44).

Variable	n	Median RFS (months)	Univariate analysis[a] RR (95% CI)	P-value
Age (years)				
≥75	6	19.6	0.70 (0.17-2.02)	0.543
<75	38	16.6		
Sex				
Male	28	16.6	2.32 (0.98-6.38)	0.056
Female	16	NR		
Body mass index (kg/m^2)				
≥25	8	16.6	1.19 (0.40-2.92)	0.736
<25	36	20.2		
Local tumor extent				
Potentially resectable	15	14.4	1.11 (0.48-2.43)	0.794
Borderline resectable	29	18.5		
Tumor location				
Head	28	18.5	0.93 (0.43-2.13)	0.860
Body and tail	16	16.6		
Clinical tumor size (mm)				
≥20	24	13.6	1.64 (0.76-3.68)	0.209
<20	20	21.1		
CA-9 before NAT (IU/ml)				
≥37	28	18.5	1.22 (0.56-2.88)	0.625
<37	16	21.1		
Neoadjuvant therapy				
NAC+RT	23	18.5	0.93 (0.42-2.02)	0.849
NAC	21	16.3		
Pathological tumor size (mm)				
≥20	32	16.6	1.94 (0.78-5.83)	0.157
<20	12	28.5		
Lymph node metastasis				
Positive	15	16.3	1.74 (0.77-3.80)	0.175
Negative	29	20.2		
Lymphatic invasion				
Positive	23	16.3	1.05 (0.48-2.28)	0.912
Negative	21	18.5		
Vascular invasion				
Positive	35	16.6	1.13 (0.44-2.59)	0.779
Negative	9	20.2		
Perineural invasion				
Positive	38	18.0	2.93 (0.86-18.40)	0.093
Negative	6	NR		
CAP criteria				
Grade 1, 2	20	21.1	0.56 (0.25-1.25)	0.156
Grade 3	24	14.4		
Evans criteria				
Grade 1	15	21.1	0.87 (0.40-2.53)	0.866
Grade 2, 3	29	18.0		
Histological necrosis				
Positive	15	9.4	6.40 (2.68-15.62)	<0.001
Negative	29	28.5		
Histological large necrosis				
Positive	11	5.9	17.35 (5.71-58.92)	<0.001
Negative	33	25.0		

[a]Cox proportional hazards regression model. Upon univariate analysis, necrosis was considered a prognostic factor. P-values representing significant differences are indicated in bold print. RFS, relapse-free survival; NAT, neoadjuvant therapy; CI, confidence interval; RR, risk ratio; CA-9, carbonic anhydrase 9; RT, radiotherapy; CAP, College of American Pathologists.

pancreatic cancer (18). Second, the present study was designed to include only patients who underwent radical surgery; therefore, some patients who failed to complete NAT because of disease progression were not included. Patients who failed to complete NAT might have factors associated with a poor prognosis, such as HTN, lymph node metastasis, lymphatic invasion, venous invasion, and neural invasion. Thus, there might be a potential bias in the treatment choice of whether to perform UFS or NAT after radical surgery.

Many prognostic factors in pancreatic cancer without NAT were reported, and these prognostic factors were re-evaluated in patients with NAT in the present study (13,19-22). The present results suggest that some of the robust prognostic factors in the UFS group do not hold in the NAT group. For example, in the UFS group, lymph node metastasis and HTN were independent predictors of DSS and RFS on multivariate risk analyses (Tables SII and SIII). However, lymph node metastasis was not associated with DSS and RFS in the NAT group in the present study (Tables III and IV). In this way, prognostic factors in the UFS group might be changed after NAT and interfere with the prediction of clinical outcomes in the NAT group. Similar problems in tumors originating from other organs were reported in a previous study (19), and risk stratification of pancreatic cancer in patients with NAT should be distinctively established in the future. In the case of HTN, we previously reported that HTN was strongly associated with a poor prognosis in patients without NAT (5), and its utility was successfully extended for the NAT group in the present study.

Resistance to chemotherapy and/or radiotherapy was strongly associated with a hypoxic tumor microenvironment. Previous studies reported that a gemcitabine-induced hypoxic tumor microenvironment is associated with chemo-resistance (23,24). Thus, various therapeutic agents have been proposed to target the hypoxic tumor microenvironment in pancreatic cancer (25-27). Pathologically, Hiraoka *et al* reported that a hypoxic tumor microenvironment is closely associated with HTN in patients without NAT (7), and the present study also confirmed the significant correlations between HTN and CA-9 expression in both the UFS and NAT groups. In addition, CA-9 expression in cancer cells was upregulated after NAT in the entire patient cohort. Therefore, tumor hypoxia may also be increased by preoperative treatment. Further, CA-9 expression was higher in patients with HTN than in those without HTN in the UFS group, and it was not significantly upregulated after NAT in the subgroup analysis of patients with HTN. These results suggest that the hypoxic tumor microenvironment was already formed around HTN in pancreatic cancer before NAT, and the hypoxic microenvironment cannot be improved by NAT. Summarizing the above results, tumor hypoxia is increased in pancreatic cancer with HTN. Particularly in cases without HTN, NAT increases tumor hypoxia. These results are consistent with previous reports and may support the development of treatments using concomitant hypoxia-alleviating therapy and conventional chemotherapy.

We previously reported that HTN can be detected as poorly enhanced areas (PEAs) on preoperative computed tomography, and the presence of PEAs was found to be associated with a poor prognosis of resectable pancreatic cancer in the UFS group (5). In addition to the potential prediction of patient prognosis, PEAs may represent tumor hypoxia and subsequent resistance to NAT without the need for histological examination. Sugimoto *et al* reported that only 42% of the patients planned for NAT followed by surgery were able to undergo subsequent surgical resection, mainly due to disease progression during NAT (3). Therefore, use of PEAs to survey tumor physiological conditions and drug resistance in pancreatic cancer, as well as predict drug resistance before NAT, should be investigated.

The main limitation of the present work is that it was a single-institute, retrospective study with a relatively small number of patients undergoing NAT. In particular, it was difficult to demonstrate a significant difference in the Kaplan-Meier curves among the three groups according to the size of necrosis because only 4 patients with small necrosis were included. Thus, the results should be validated in a larger-scale study. Another limitation of this study is that it was difficult to evaluate the histological change associated with NAT and surgery. Tumor necrosis is sometimes associated with therapy and sometimes not, but it is difficult to distinguish the original HTN from the HTN that occurred as the result of therapy. Moreover, autolysis, which is caused by ischemia with surgical procedures, potentially affects the histological assessment of tumor necrosis. This was a retrospective study, and there was no precise protocol for management of fresh surgical samples. The impact of NAT and surgical procedures on histological changes in pancreatic cancer would be the next subject to examine in future studies. The last limitation of this study is related to the mechanism of HTN generation. As far as we know, the basic mechanisms of HTN generation in pancreatic cancer are still unclear. Further basic investigation is needed to establish novel treatments targeting HTN and the hypoxic microenvironment.

In conclusion, HTN is a robust prognostic marker in pancreatic cancer patients after NAT. Furthermore, the results suggest a close association between HTN and tumor hypoxia and may support the concomitant use of hypoxia-alleviating therapy before or together with NAT. Clinical detection of HTN is a potential biomarker of prognosis and therapeutic response in pancreatic cancer patients.

Acknowledgements

The authors would like to thank all participating patients and their families who made this study possible.

Funding

This research did not receive any specific grant from funding agencies in the public, commercial, or not-for-profit sectors.

Availability of data and materials

The datasets generated and/or analyzed during the present study are available from the corresponding author upon reasonable request.

Authors' contributions

MKudo designed the study and wrote the initial draft of the manuscript. MKudo contributed to analysis and interpretation

of the data and assisted in the preparation of the manuscript. GI, NG, MKonishi, ST, SK, MS, JDM, HC, and MKojima contributed to data collection and interpretation and critically reviewed the manuscript. All authors approved the final version of the manuscript and agree to be accountable for all aspects of the work in ensuring that questions related to the accuracy or integrity of any part of the work (in addition to the data provided) are appropriately investigated and resolved.

Ethics approval and consent to participate

Patient tissue samples were collected between 2011 and 2019 at the Department of Pathology, National Cancer Center Hospital East, Kashiwa, Japan. This study protocol conformed to the ethical guidelines of the 1975 Declaration of Helsinki and was approved by the Institutional Review Board of the National Cancer Center, Japan (reference 2017-328), and informed consent was obtained from all patients.

Patient consent for publication

Not applicable.

Competing interests

John D. Martin is an employee of NanoCarrier Co., Ltd. The other authors have no competing interests.

References

1. Siegel RL, Miller KD and Jemal A: Cancer statistics, 2018. CA Cancer J Clin 68: 7-30, 2018.
2. Zhan HX, Xu JW, Wu D, Wu ZY, Wang L, Hu SY and Zhang GY: Neoadjuvant therapy in pancreatic cancer: A systematic review and meta-analysis of prospective studies. Cancer Med 6: 1201-1219, 2017.
3. Sugimoto M, Takahashi N, Farnell MB, Smyrk TC, Truty MJ, Nagorney DM, Smoot RL, Chari ST, Carter RE and Kendrick ML: Survival benefit of neoadjuvant therapy in patients with non-metastatic pancreatic ductal adenocarcinoma: A propensity matching and intention-to-treat analysis. J Surg Oncol 120: 976-984, 2019.
4. Unno M, Hata T and Motoi F: Long-term outcome following neoadjuvant therapy for resectable and borderline resectable pancreatic cancer compared to upfront surgery: A meta-analysis of comparative studies by intention-to-treat analysis. Surg Today 49: 295-299, 2019.
5. Kudo M, Kobayashi T, Gotohda N, Konishi M, Takahashi S, Kobayashi S, Sugimoto M, Okubo S, Martin J, Cabral H, *et al*: Clinical utility of histological and radiological evaluations of tumor necrosis for predicting prognosis in pancreatic cancer. Pancreas 49: 634-641, 2020.
6. Mitsunaga S, Hasebe T, Iwasaki M, Kinoshita T, Ochiai A and Shimizu N: Important prognostic histological parameters for patients with invasive ductal carcinoma of the pancreas. Cancer Sci 96: 858-865, 2005.
7. Hiraoka N, Ino Y, Sekine S, Tsuda H, Shimada K, Kosuge T, Zavada J, Yoshida M, Yamada K, Koyama T and Kanai Y: Tumour necrosis is a postoperative prognostic marker for pancreatic cancer patients with a high interobserver reproducibility in histological evaluation. Br J Cancer 103: 1057-1065, 2010.
8. Okusaka T, Nakamura M, Yoshida M, Kitano M, Uesaka K, Ito Y, Furuse J, Hanada K and Okazaki K: Clinical practice guidelines for pancreatic cancer 2019 from the Japan Pancreas Society: A synopsis. Pancreas 49: 326-335, 2020.
9. Takahashi S: How to treat borderline resectable pancreatic cancer: Current challenges and future directions. Jpn J Clin Oncol 48: 205-213, 2018.
10. Motoi F, Kosuge T, Ueno H, Yamaue H, Satoi S, Sho M, Honda G, Matsumoto I, Wada K, Furuse J, *et al*: Randomized phase II/III trial of neoadjuvant chemotherapy with gemcitabine and S-1 versus upfront surgery for resectable pancreatic cancer (Prep-02/JSAP05). Jpn J Clin Oncol 49: 190-194, 2019.
11. Takahashi S, Ohno I, Ikeda M, Kobayashi T, Akimoto T, Kojima M, Konishi M and Uesaka K: Neoadjuvant S-1 with concurrent radiotherapy followed by surgery for borderline resectable pancreatic cancer: Study protocol for an open-label, multicentre, prospective phase II trial (JASPAC05). BMJ Open 7: e018445, 2017.
12. Takahashi S, Ohno I, Ikeda M, Konishi M, Kobayashi T, Akimoto T, Kojima M, Morinaga S, Toyama H, Shimizu Y, *et al*: Neoadjuvant S-1 with concurrent radiotherapy followed by surgery for borderline resectable pancreatic cancer: A phase II open-label multicenter prospective trial (JASPAC05). Ann Surg: Oct 15, 2020 (Epub ahead of print). doi: 10.1097/SLA.0000000000004535.
13. Okubo S, Kojima M, Matsuda Y, Hioki M, Shimizu Y, Toyama H, Morinaga S, Gotohda N, Uesaka K, Ishii G, *et al*: Area of residual tumor (ART) can predict prognosis after post neoadjuvant therapy resection for pancreatic ductal adenocarcinoma. Sci Rep 9: 17145, 2019.
14. Brierley JD, Gospodarowicz MK and Wittekind C: TNM Classification of Malignant Tumours. John Wiley and Sons, 2017.
15. N Kalimuthu S, Serra S, Dhani N, Hafezi-Bakhtiari S, Szentgyorgyi E, Vajpeyi R and Chetty R: Regression grading in neoadjuvant treated pancreatic cancer: An interobserver study. J Clin Pathol 70: 237-243, 2017.
16. Evans DB, Rich TA, Byrd DR, Cleary KR, Connelly JH, Levin B, Charnsangavej C, Fenoglio CJ and Ames FC: Preoperative chemoradiation and pancreaticoduodenectomy for adenocarcinoma of the pancreas. Arch Surg 127: 1335-1339, 1992.
17. Aperio Positive Pixel Count Algorithm. Journal 2020.
18. Mirkin KA, Greenleaf EK, Hollenbeak CS and Wong J: Correlation of clinical and pathological staging and response to neoadjuvant therapy in resected pancreatic cancer. Int J Surg 52: 221-228, 2018.
19. Sakuyama N, Kojima M, Kawano S, Matsuda Y, Mino-Kenudson M, Ochiai A and Ito M: Area of residual tumor is a robust prognostic marker for patients with rectal cancer undergoing preoperative therapy. Cancer Sci 109: 871-878, 2018.
20. Kawai M, Hirono S, Okada KI, Miyazawa M, Shimizu A, Kitahata Y, Kobayashi R, Ueno M, Hayami S, Tanioka K and Yamaue H: Low lymphocyte monocyte ratio after neoadjuvant therapy predicts poor survival after pancreatectomy in patients with borderline resectable pancreatic cancer. Surgery 165: 1151-1160, 2019.
21. Lei MZ, Li XX, Zhang Y, Li JT, Zhang F, Wang YP, Yin M, Qu J and Lei QY: Acetylation promotes BCAT2 degradation to suppress BCAA catabolism and pancreatic cancer growth. Signal Transduct Target Ther 5: 70, 2020.
22. Zheng Y, Wu C, Yang J, Zhao Y, Jia H, Xue M, Xu D, Yang F, Fu D, Wang C, *et al*: Insulin-like growth factor 1-induced enolase 2 deacetylation by HDAC3 promotes metastasis of pancreatic cancer. Signal Transduct Target Ther 5: 53, 2020.
23. Arora S, Bhardwaj A, Singh S, Srivastava SK, McClellan S, Nirodi CS, Piazza GA, Grizzle WE, Owen LB and Singh AP: An undesired effect of chemotherapy: Gemcitabine promotes pancreatic cancer cell invasiveness through reactive oxygen species-dependent, nuclear factor κB- and hypoxia-inducible factor 1α-mediated up-regulation of CXCR4. J Biol Chem 288: 21197-21207, 2013.
24. Däster S, Amatruda N, Calabrese D, Ivanek R, Turrini E, Droeser RA, Zajac P, Fimognari C, Spagnoli GC, Iezzi G, *et al*: Induction of hypoxia and necrosis in multicellular tumor spheroids is associated with resistance to chemotherapy treatment. Oncotarget 8: 1725-1736, 2017.
25. Hoang NT, Kadonosono T, Kuchimaru T and Kizaka-Kondoh S: Hypoxia-inducible factor-targeting prodrug TOP3 combined with gemcitabine or TS-1 improves pancreatic cancer survival in an orthotopic model. Cancer Sci 107: 1151-1158, 2016.
26. Shannon AM, Bouchier-Hayes DJ, Condron CM and Toomey D: Tumour hypoxia, chemotherapeutic resistance and hypoxia-related therapies. Cancer Treat Rev 29: 297-307, 2003.
27. Chauhan VP, Martin JD, Liu H, Lacorre DA, Jain SR, Kozin SV, Stylianopoulos T, Mousa AS, Han X, Adstamongkonkul P, *et al*: Angiotensin inhibition enhances drug delivery and potentiates chemotherapy by decompressing tumour blood vessels. Nat Commun 4: 2516, 2013.